Measurements of Intracellular Mg^{2+} Concentration in Mouse Skeletal Muscle Fibers with the Fluorescent Indicator Mag-Indo-1

Laszlo Csernoch,* Jean Claude Bernengo,# Peter Szentesi,* and Vincent Jacquemond§

*Department of Physiology, University Medical School of Debrecen, H-4012 Debrecen, Hungary; #INSERM U121, 69500 Bron, France; and §Laboratoire de Physiologie des Eléments Excitables, Université Claude Bernard Lyon 1, UMR CNRS 5578, F69622 Villeurbanne, France

ABSTRACT Measurements of intracellular free magnesium concentration ($[Mg^{2+}]_i$) were performed on enzymatically isolated skeletal muscle fibers from mice, using the fluorescent ratiometric indicator mag-indo-1. An original procedure was developed to calibrate the dye response within the fibers: fibers were first permeabilized with saponin in the presence of a given extracellular magnesium concentration and were then embedded in silicone grease. The dye was then pressure microinjected into the saponin-permeabilized silicone-embedded fibers, and fluorescence was measured. The results show that for all tested $[Mg^{2+}]$, the value of the measured fluorescence ratio was higher than that found in aqueous solutions. Furthermore, the apparent binding curve that could be fit to the in vivo ratio data was shifted toward higher $[Mg^{2+}]$ by a factor of ~2. Using the in vivo calibration parameters, the mean resting $[Mg^{2+}]_i$ was found to be 1.53 ± 0.16 mM ($n = 7$). In an attempt to gain insight into the myoplasmic magnesium buffering capacity, we measured, together with mag-indo-1 fluorescence, the current elicited by the application of carbamylcholine (CCh) to the endplate of isolated fibers, in the presence of a high extracellular magnesium concentration. The results show that, under these conditions, a change in $[Mg^{2+}]_i$ displaying a time course and amplitude qualitatively consistent with the CCh-induced inward current can be measured.

INTRODUCTION

In most cell types, the intracellular free magnesium level is likely to play a key role in numerous physiological processes (for a review, see Romani and Scarpa, 1992). In skeletal muscle, the regulation of the overall excitation-contraction coupling process is undoubtedly dependent on the cytoplasmic free magnesium concentration ($[Mg^{2+}]_i$), because, apart from its effects on the contractile machinery (for a review, see Potter et al., 1981), calcium uptake by myoplasmic calcium buffers (Gillis et al., 1982; Hou et al., 1991) and sarcoplasmic reticulum (SR) (e.g., Kabbara and Stephenson, 1994), magnesium could modulate the activity of various ionic channels present in the surface membrane (Agus and Morad, 1991). It is also strongly suspected to play a direct role in the regulation of the depolarization-induced SR calcium release process (Stephenson, 1981; Lamb and Stephenson, 1991; Jacquemond and Schneider, 1992b). Although previous studies using antipyrylazo III as a magnesium indicator showed that changes in $[Mg^{2+}]_i$ related to excitation-contraction coupling can be measured (Irving et al., 1989; Bernengo et al., 1992; Jacquemond and Schneider, 1992a), there seems to be a general agreement that changes in $[Mg^{2+}]_i$ cannot have a "trigger" role, as is widely recognized for changes in intracellular free calcium for many cellular processes.

Previous measurements of the resting $[Mg^{2+}]_i$ in skeletal muscle cells by different methods gave a quite broad range of values (for instance, 0.2–5 mM in frog skeletal muscle; see Romani and Scarpa, 1992), which appears to be due primarily to technical difficulties in accurately and specifically measuring free magnesium in intact cells. This is also probably the main reason why very little is known about the regulation of intracellular free magnesium as compared to calcium.

Using the ratiometric fluorescent indicator mag-indo-1, we performed experiments aimed at estimating the $[Mg^{2+}]_i$ in isolated skeletal muscle fibers from mice and at determining the extent to which the resting $[Mg^{2+}]_i$ can be increased by magnesium influx from the extracellular medium. Such measurements inevitably required first an intracellular calibration of the dye response versus the magnesium concentration, because the fluorescence properties and apparent affinity of the dye for magnesium might be affected by the intracellular environment as compared to in vitro, as suggested for furaptra (Konishi et al., 1993). Finally, we took advantage of the known significant permeability of the endplate nicotinic receptors to magnesium ions (Adams et al., 1980; Manthey, 1995) to achieve simultaneous measurements of a magnesium influx across the plasma membrane and a subsequent increase in $[Mg^{2+}]_i$. A preliminary account of some of this work has been presented to the Biophysical Society (Csernoch et al., 1996).

MATERIALS AND METHODS

The methods used here for $[Mg^{2+}]$ measurements were similar to those previously described for $[Ca^{2+}]$ measurements of the same preparation (Allard et al., 1996; Jacquemond, 1997). In the present work, however,

Received for publication 4 February 1998 and in final form 30 April 1998.

Address reprint requests to Dr. Vincent Jacquemond, Laboratoire de Physiologie des Eléments Excitables, Université Claude Bernard, Lyon 1, Bât. 401 B, 43 boulevard du 11 novembre 1918, F 69622 Villeurbanne Cedex, France. Tél.: 33-4-72-43-10-32; Fax: 33-4-78-94-68-20; E-mail: jacquemo@physio.univ-lyon1.fr.

0006-3495/98/08/967/11 $2.00

mag-indo-1 was used in place of indo-1 as the fluorescent indicator, except for one experiment, the results of which are presented in Fig. 6.

Isolation and preparation of the muscle fibers for the fluorescence measurements

Experiments were performed on intact skeletal fibers from the flexor digitorum brevis muscles of mice. Single fibers were isolated from collagenase (Sigma type 1)-treated muscles as previously described (Allard et al., 1996). Intracellular dye loading was performed by local pressure microinjection of a solution containing mag-indo-1 (pentapotassium salt; Molecular Probes, Eugene, OR) at a concentration of 1–2 mM, with a Picospritzer II apparatus (General Valve Corp., Fairfield, NJ). In some cases, the solution that was microinjected contained EGTA or ATP (details are given below). The final concentration of mag-indo-1 within the injected fibers was approximated by first measuring the length of the portion of fiber that appeared fluorescent right after the end of the injection, and dividing it by the total length of the fiber. The concentration of dye after diffusion was complete was then calculated by scaling the concentration in the injection solution by this ratio. This calculated value actually represents an upper limit for the final dye concentration, because it is assumed that, right after injection, the dye concentration within the fluorescent portion of fiber was homogeneous and equal to the concentration in the pipette. This was certainly not true, because as typical injections always lasted for ~30 s, when the length of the fluorescent portion of fiber was measured, some dye had already diffused along the fiber. Of 67 fibers that were injected with mag-indo-1, the mean injected volume calculated this way represented 13.5 ± 1% of the total volume of fiber, and the mean (maximum) final dye concentration was 210 ± 10 μM.

The procedures that we used for the in vivo calibration of the fluorescence and for the endplate current measurements (see corresponding sections in the text) required the isolated fibers to be entirely or partly embedded in silicone grease, respectively (Jacquemond, 1997). For this, the bottom of the experimental chamber, which consisted of a glass coverslip, had to be first covered with a thin layer of silicone. The chamber was then filled with culture medium containing 10% bovine fetal serum (MI199; Eurobio, Les Ulis, France), and the collagenase-treated muscles were gently triturated within the chamber through the cut disposable tip of a Pipetman. As previously reported (Jacquemond, 1997), the presence of culture medium during that step was necessary to protect the fibers from being damaged upon contact with the silicone. After ~10 min, the culture medium was replaced with the external solution, the composition of which depended on the type of measurements that were done (see sections Calibration and Electrophysiology).

The mean values of resting $[Mg^{2+}]_i$ reported here were obtained from fibers that were not handled with the silicone grease, but were simply left to settle on the bottom of the experimental chamber, which, in that case, was coated with poly-L-lysine as described previously (Allard et al., 1996). In one series of measurements, the extracellular medium consisted of a regular Tyrode solution containing (in mM) 140 NaCl, 5 KCl, 2.5 $CaCl_2$, 1 $MgCl_2$, 10 HEPES, adjusted to pH 7.40 with NaOH, and the solution that was microinjected contained (in mM) 140 K-aspartate, 2 EGTA, 1 mag-indo-1, 6 HEPES, adjusted to pH 7.20 with KOH. In another series of measurements, the extracellular solution contained (in mM) 135 NaCl, 1 $MgCl_2$, 10 EGTA, 10 HEPES, adjusted to pH 7.20 with NaOH, and the solution that was microinjected contained (in mM) 140 K-aspartate, 10 EGTA, 1 mag-indo-1, 5 HEPES, adjusted to pH 7.20 with KOH.

Optical apparatus and $[Mg^{2+}]$ calculation from the fluorescence signals

The diafluorescence optical set-up used for mag-indo-1 fluorescence measurements was described previously (Allard et al., 1996). The beam of light, from a high-pressure mercury bulb set on the top of a Nikon Diaphot epifluorescence microscope, was passed through a 335-nm interference filter providing the excitation light for mag-indo-1 and focused on the preparation through a quartz aspherical doublet. The emitted fluorescence light was collected by the 40× objective and detected at 405 (F_{405}) and 470 nm (F_{470}) with a 10-nm bandwidth by two photomultipliers. Fluorescence signals were digitized and stored on disk with commercial software (Biopatch Acquire; Bio-logic, Claix, France) driving an A/D, D/A converter (Lab Master DMA board; Scientific Solutions, Solon, OH). The fluorescence measurement field was 40 μm in diameter. Mag-indo-1 microinjected fibers were only UV illuminated while measurements were taken, to minimize photobleaching. Cell autofluorescence was found to be negligible and not different from the fluorescence measured when no cell was present in the field. Background fluorescence at both emission wavelengths was thus measured next to each tested fiber and then subtracted from all measurements.

The $[Mg^{2+}]$ was estimated from the ratio (R) of the background corrected fluorescence at 405 and 470 nm (F_{405}/F_{470}), using the standard procedure developed by Grynkiewicz et al. (1985), with the parameters R, R_{min} (R in the absence of Mg), R_{max} (R in the presence of a saturating Mg concentration), K_D (the apparent binding constant for the mag-indo-1-Mg complex), and β (the ratio of F_{470} in the absence of Mg and F_{470} in the presence of a saturating Mg concentration).

In vitro and in vivo calibrations of the mag-indo-1 response

In vitro calibrations were performed on the experimental set-up using glass capillary tubes, 50 μm in diameter, filled with magnesium calibrating solutions containing 0.05 mM mag-indo-1 (pentapotassium salt; Molecular Probes, Eugene, OR). The calibrating solutions were prepared by mixing in different ratios two stock solutions containing (in mM) 150 KCl, 1 EGTA, 10 HEPES, and 100 $MgCl_2$, 1 EGTA, 10 HEPES (pH adjusted to 7.20 with KOH), respectively, so as to achieve various concentrations of Mg^{2+}. A so-called 0.01 mM $[Mg^{2+}]$ solution was also made by adding 1.6 mM ATP to the stock solution containing no $MgCl_2$, assuming the Mg contamination from the KCl salt to be 0.05% and the apparent affinity of ATP for Mg to be 0.1 mM. Fig. 1 shows the results of the tube calibration. The fluorescence at 405 nm and 470 nm is shown in Fig. 1 *A* as a function of $[Mg^{2+}]$, and the corresponding ratio values are shown in Fig. 1 *B*. Fig. 1 *A* demonstrates that an increase in $[Mg^{2+}]$ produces an increase in F_{405} and not much of a change in F_{470}, in agreement with 470 nm being close to the isoemissive point of the fluorescence spectrum (Haugland, 1996), and thus that the value of the β factor should be close to 1. Result from fitting a 1:1 binding curve to the F_{405} data points is shown as the superimposed solid curve; this gave an apparent affinity K_D = 5.1 mM. In Fig. 1 *B*, the solid curve superimposed on the ratio data corresponds to the result of fitting the 1:1 binding, which gave R_{min} = 0.20, R_{max} = 1.55, and $K_D \cdot \beta$ = 5.43 mM.

Because the fluorescence measurements for the in vivo calibrations were performed on cells that were embedded in silicone grease, we performed a series of in vitro measurements with the tubes completely embedded in silicone grease, to detect a possible difference that would be introduced in the fluorescence ratio. Results showed that for all $[Mg^{2+}]$, the values of the fluorescence ratio were identical to those shown in Fig. 1 *B*.

In vivo calibrations were performed using the same solutions as used for the tube measurements, except for the lowest $[Mg^{2+}]$ (R_{min} measurements). Equilibration of intracellular $[Mg^{2+}]$ was achieved by transiently treating the fibers with saponin to permeabilize the membrane of the fibers. To avoid the difficulties related to dye leaking out of the permeabilized fibers (see Results), we designed a protocol involving complete embedding of the saponin treated fibers in silicone grease, to keep the dye inside the cell. The overall procedure took several steps:

1. A batch of isolated fibers was left sitting on a silicone layer covering the bottom of the experimental chamber for ~10 min, in the presence of culture medium as extracellular solution.

2. The culture medium was replaced by one of the magnesium calibrating solutions.

3. The extracellular calibrating solution was then replaced by the same solution, also containing 0.02% saponin.

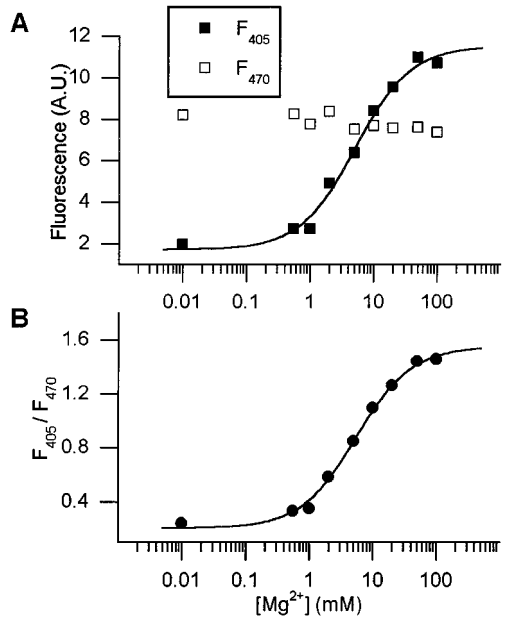

FIGURE 1 In vitro calibration of mag-indo-1 fluorescence. (*A*) Fluorescence of mag-indo-1 versus $[Mg^{2+}]$. Fluorescence at 405 (■) and 470 nm (□) in arbitrary units (A.U.) was measured from glass capillary tubes filled with $[Mg^{2+}]$ calibrated solutions containing 0.05 mM mag-indo-1. (*B*) Ratio of the mag-indo-1 fluorescence at 405 and 470 nm versus $[Mg^{2+}]$. The result from fitting a 1:1 binding curve to the F_{405} data points (*A*) and to the ratio values (*B*) is shown as a superimposed curve.

4. The saponin-containing solution was replaced with the magnesium calibrating solution (no saponin, same as in second step). The total time during which fibers were in contact with saponin was always ~5 min.

5. A few fibers were then completely covered with silicone grease, which was performed by applying pressure through a silicone-filled glass micropipette with a broken tip, using the Picospritzer apparatus.

6. The silicone-embedded fibers were then pressure microinjected with mag-indo-1 (2 mM in deionized water); the dye was injected locally, with the tip of the injecting microelectrode inserted within the fibers through the silicone. After dye diffusion throughout the volume of the fibers, four or five fluorescence measurements were taken at different locations along each injected fiber. Once a fiber was covered with silicone and the dye had equilibrated throughout the fiber, the only limitation to obtaining a stable fluorescent signal was photobleaching of the dye; otherwise stable fluorescent signals could be recorded for hours.

For measurements of R_{min}, fibers were treated with saponin as described above, in the presence of a solution containing (in mM) 120 KCl, 50 EDTA, 10 HEPES, and 1 EGTA (pH adjusted to 7.20 with KOH) before being completely embedded in silicone grease. Fibers were then pressure microinjected with a solution containing (in mM) 100 K aspartate, 30 K_2-ATP, 1 EGTA, 5 piperazine-*N,N′*-bis(2-ethanesulfonic acid) (PIPES), and 1 mag-indo-1 (pH 7.20).

The R_{max} value was checked in fibers that were not treated with saponin but directly embedded in silicone grease and pressure microinjected with mag-indo-1 (2 mM in deionized water). After dye equilibration, a second microinjection was performed with the micropipette containing a 4.9 M $MgCl_2$ solution. Fluorescence was measured until a steady level was reached.

Electrophysiology

Carbamylcholine (CCh)-induced endplate current measurements were carried out by a method previously described (Jacquemond, 1997). Single isolated fibers were embedded in silicone grease so that only a portion including the endplate area was in contact with the extracellular solution. Care was taken that the endplate was sitting on the top surface of the tested fibers. Membrane current was measured with a single microelectrode in connection with a patch-clamp amplifier in whole-cell mode (RK300; Bio-logic). Microelectrodes were filled with a solution containing K acetate (3 M) and KCl (20 mM) and had a resistance ranging between 1 and 3 MΩ. The tip of the microelectrode was inserted through the silicone, within the insulated portion of the fiber. The holding command potential was set to −80 mV (unless otherwise specified in the text). The tested cells were superfused with an extracellular solution containing (in mM) 100 $MgSO_4$, 100 mannitol, 10 HEPES (pH 7.20), or 130 $MgSO_4$, 10 $MgCl_2$, 10 PIPES, 5 EGTA (pH 7.20). Superfusion of the extracellular solution in the vicinity of each tested cell was achieved by using a thin polyethylene capillary perfusion system operating by gravity. Endplate currents were elicited by applying CCh puffs to the endplate with a micropipette with a blunt tip filled with 10 mM CCh dissolved in the same solution as the extracellular one. CCh puffs were delivered by pressure pulses applied through the micropipette with the Picospritzer apparatus. The tip of the micropipette was always positioned less than 30 μm from the endplate.

Statistics

Least-squares fits were performed with a Marquardt-Levenberg algorithm routine included in Microcal Origin (Microcal Software, Northampton, MA). Data values are presented as means ± SEM.

RESULTS

In vivo calibration of the mag-indo-1 response

In a first series of trials, we tested the effect of an application of saponin to mag-indo-1 microinjected fibers, in the presence of a given $[Mg^{2+}]$ calibrating solution as extracellular medium. Fig. 2 shows the result of such an experiment. The mag-indo-1 microinjected fiber was superfused with a solution containing (in mM) 50 $MgCl_2$, 10 EGTA, 10 HEPES (pH 7.20), and the fluorescence at both wavelengths was continuously monitored. At the time indicated by the arrow, a 5-s puff of saponin (0.01%, dissolved in the same solution as the superfused one) was applied directly to the portion of fiber from which fluorescence was measured, using a micropipette connected to the Picospritzer apparatus. Saponin initially induced a transient increase in F_{405}, while F_{470} started to simultaneously decrease, then the fluorescence rapidly and strongly decreased at both wavelengths. The initial increase and simultaneous decrease in F_{405} and F_{470}, respectively, produced an increase in the ratio that was likely due to an increase in intracellular magnesium. The nonspecific membrane-permeabilizing effect of saponin was most likely responsible for the dye leaking out of the cell and the consequent loss of fluorescence, which rendered the accuracy of the fluorescence ratio estimation uncertain at later times.

Fig. 3 shows the overall results of the in vivo calibration performed on fibers permeabilized with saponin and subsequently embedded in silicone grease as described in Materials and Methods. A 1:1 binding function was fitted to the data points and is shown as a superimposed solid curve. The fit was forced through the mean R_{min} value (0.41 ± 0.03) obtained from six fibers treated as described in Materials and Methods, and the corresponding $[Mg^{2+}]$ was arbitrarily

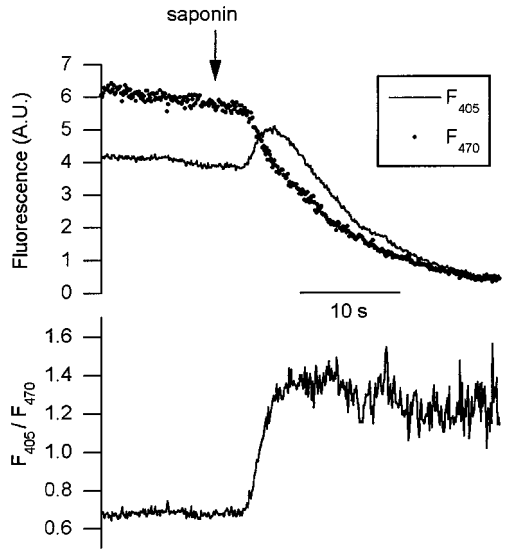

FIGURE 2 Effect of applying saponin, in the presence of a high extracellular [Mg^{2+}], to a fiber microinjected with mag-indo-1. (*Top*) Two traces corresponding to the fluorescence simultaneously measured at 405 (——) and 470 nm (·····), respectively. The fiber was superfused with a solution containing 50 mM $MgCl_2$. At the time indicated by the arrow, saponin (0.01%) was puffed onto the portion of the fiber from which fluorescence was measured. (*Bottom*) The ratio of F_{405} and F_{470}, calculated from the fluorescence traces shown above. The injected solution contained (in mM) 140 K-aspartate, 10 EGTA, 1 mag-indo-1, 5 HEPES (pH 7.20).

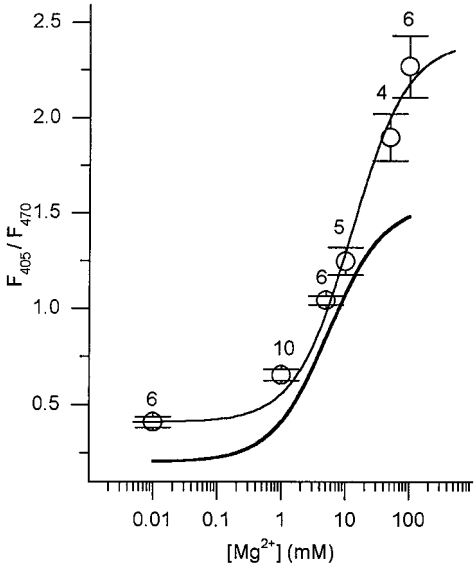

FIGURE 3 In vivo calibration of mag-indo-1 fluorescence. Data points correspond to the mean ± SEM ratio of fluorescence at 405 and 470 nm. They were calculated from fluorescence measurements performed on fibers transiently treated with saponin in the presence of a given extracellular [Mg^{2+}] calibrating solution before being completely embedded within silicone and pressure microinjected with mag-indo-1 (for details, see corresponding section in Materials and Methods). The number of fibers is indicated above each data point. The superimposed solid line corresponds to the result from fitting a 1:1 binding curve to the in vivo data points. For comparison, the fit obtained from the in vitro data points is presented on the same graph as a dotted curve.

set to 0.01 mM. Changing this value to 0.001 or 0.05 mM did not influence the fit. The fit gave values of 12.5 mM and 2.40 for $K_D \cdot \beta$ and R_{max}, respectively. The value of R_{max} from the fit was close to the mean value obtained from a number of fibers pressure microinjected using a very high $MgCl_2$ concentration in the pipette as described in Materials and Methods ($R_{max} = 2.33 \pm 0.13$, $n = 5$). To facilitate the comparison with the in vitro data, the result of the fit from the tube measurements is also shown in Fig. 3 as a dotted curve. It clearly appears that for all [Mg^{2+}], the values of the fluorescence ratio were larger in vivo than in vitro. Furthermore, the in vivo relationship between the ratio and the [Mg^{2+}] was shifted toward higher [Mg^{2+}] as compared to that in vitro. Such discrepancies are likely to be due to differences in the fluorescence properties of the dye and possibly to a shift in the apparent affinity of the dye for magnesium between the two sets of conditions. To clarify this point, we attempted to estimate the value of the β factor in vivo.

Fig. 4 shows fluorescence traces measured from a fiber embedded in silicone grease and pressure microinjected with mag-indo-1, and then after dye equilibration, a second microinjection was performed with the pipette containing a 4.9 M $MgCl_2$ solution. The tip of the pipette was inserted ~40 μm from the center of the fluorescence measurement area, and the pressure was kept constant throughout the recording period. Although the absolute changes in fluorescence due to the magnesium injection could be corrupted to some extent by photobleaching and a change in dye concentration, the experiment shows that during the increase in F_{405}, F_{470} decreased by a factor of ~2, which is clearly different from what was expected from the tube calibration. The corresponding fluorescence ratio shown in the bottom panel of Fig. 4 reached a value close to R_{max} in response to the increase in magnesium. The value of β can also be estimated from the slope of plots of F_{470} versus F_{405} when the [Mg^{2+}] is changing, according to the principles developed by Bakker et al. (1993) and Westerblad and Allen (1996). For an ion-sensitive ratiometric dye, assuming that the total concentration of dye is the sum of the concentrations of the ion-bound and free forms, and that the fluorescence intensity at a given wavelength is proportional to the respective contribution of the two fluorescent species, it can be shown that the fluorescence intensities at two wavelengths are linearly related (Vranesic and Knöpfel, 1991). Under our conditions, using the terminology of Bakker et al. (1993), this can be expressed as $F_{470} = m \cdot F_{405} + e$, where m and e are constants. The calibration parameter β can then be readily calculated from the slope m, and from R_{min} and R_{max} according to $\beta = (1 - m \cdot R_{max})/(1 - m \cdot R_{min})$. A plot of F_{470} versus F_{405} is shown as an inset in the top panel of Fig. 4. The least-squares fit is presented as a straight line superimposed on the data points, giving a slope of −0.99, which corresponds to a β factor equal to 2.4. Because the in vitro value of β was probably close to 1, as shown from data in Fig. 1, this approximately twofold increase could thus be

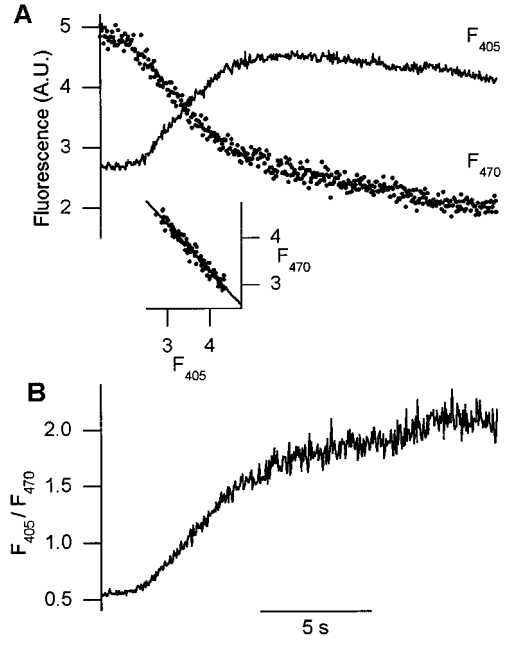

FIGURE 4 Effect of injecting a high concentration of $MgCl_2$ into a fiber previously injected with mag-indo-1. The fiber was first embedded in silicone and pressure microinjected with mag-indo-1 (2 mM in deionized water), and then, after dye equilibration, a second microinjection was performed with the pipette containing a 4.9 M $MgCl_2$ solution. (*A*) fluorescence measured throughout the $MgCl_2$ injection period at 405 nm (*solid trace*) and 470 nm (*dotted trace*), respectively. The inset shows a plot of F_{470} versus F_{405} that was fitted with a straight line (*superimposed solid curve*). (*B*) Ratio of F_{405} and F_{470}, calculated from the data shown in *A*.

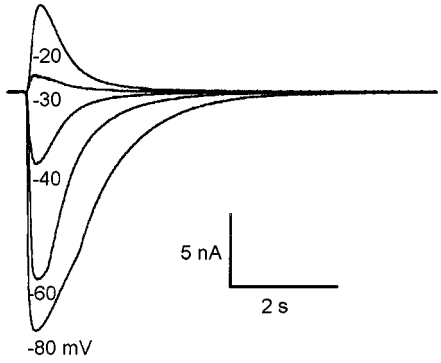

FIGURE 5 Changes in membrane current elicited by successive 100-ms CCh applications to the endplate of a fiber superfused with the 100 mM $MgSO_4$ external solution. The value of the holding command potential is indicated next to each corresponding record.

sufficient to explain the shift of the experimental binding calibration curve toward higher $[Mg^{2+}]$.

Resting $[Mg^{2+}]_i$

Using the in vivo calibration parameters, the mean resting $[Mg^{2+}]_i$ from seven fibers in the presence of extracellular Tyrode solution was 1.53 ± 0.16 mM. To check for a possible interference of the mag-indo-1 response with calcium, we performed most of the resting $[Mg^{2+}]_i$ measurements using an extracellular solution and a microinjection solution containing 10 mM EGTA (see Materials and Methods). In these conditions, the mean resting $[Mg^{2+}]_i$ was found to be 1.41 ± 0.19 mM ($n = 34$).

Simultaneous measurements of endplate current and change in $[Mg^{2+}]_i$

Fig. 5 shows a series of changes in membrane current elicited by successive 100-ms CCh applications to the endplate of a fiber superfused with the 100 mM $MgSO_4$ external solution. CCh application induced a transient inward current for a holding command potential of −80 mV. For more depolarized potentials, the amplitude of the inward current became smaller, and the current turned outward for a holding command potential of −30 mV. This value is in agreement with the theoretical reversal potential (~ −40 mV) that can be calculated from the concentration gradients of the permeant ionic species present under our experimental conditions (Na^+, K^+, Mg^{2+}), using the relative permeability values of endplate channels determined by Adams et al. (1980). The currents shown in Fig. 5 resemble those previously observed, by a two-microelectrode or a vaseline gap voltage clamp technique, for frog skeletal muscle fibers in the presence of a high external magnesium concentration (Adams et al., 1980; Manthey, 1995). It has to be stressed that, in our conditions, considering the large amplitude of the CCh-induced currents (10–20 nA), the membrane potential may have been imperfectly controlled, due in particular to the voltage drop, because of current flowing through the series resistance introduced by the microelectrode. However, because the main goal of these experiments was to achieve the measurement of an increase in $[Mg^{2+}]_i$ due to an estimated influx of Mg^{2+}, we were not so concerned about any simultaneous drop in membrane voltage, as long as it did not have any influence on the measured fluorescence signals.

The left panel of Fig. 6 shows simultaneous records of changes in membrane current and $[Mg^{2+}]_i$ elicited by a 100-ms puff of CCh to the endplate. The CCh puff produced a transient inward current, which reached a maximum amplitude of 9.4 nA 300 ms after the onset of CCh application, and then slowly decayed back to its initial level. From the mag-indo-1 fluorescence, CCh also induced an increase in $[Mg^{2+}]_i$ from a resting level of 1.1 mM up to 1.5 mM. The maximum $[Mg^{2+}]_i$ was reached ~2 s after the onset of CCh application and did not present any clear decaying phase over the recorded interval. Because mag-indo-1 is also sensitive to calcium, we considered the possibility that the observed mag-indo-1 response could be due to an increase in intracellular free calcium concentration ($[Ca^{2+}]_i$) produced by membrane depolarization due to loss of voltage control during the CCh-induced current. Regarding this possibility, it first has to be stressed that we never observed any local contractile response upon CCh application under

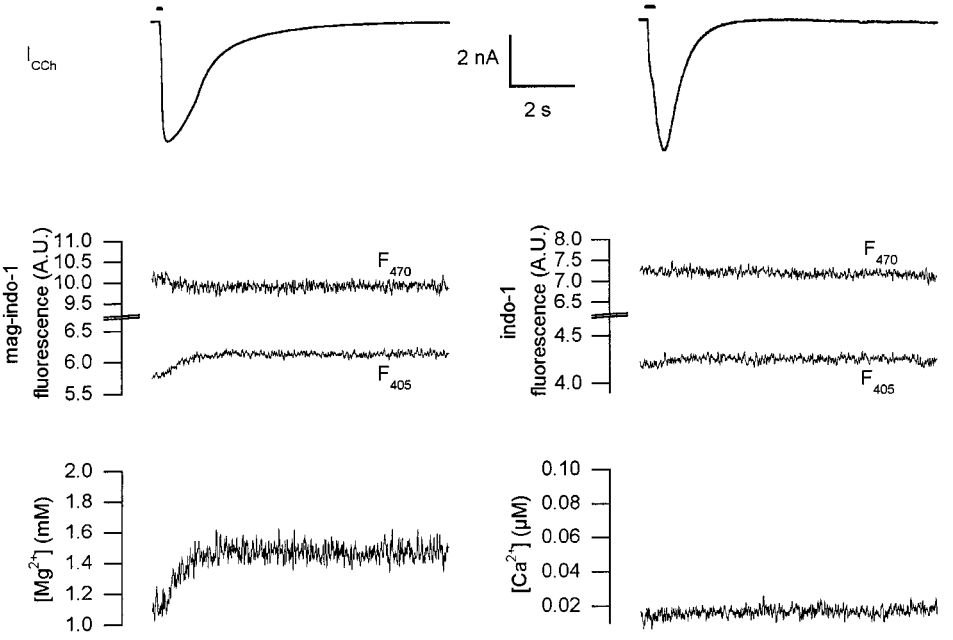

FIGURE 6 Simultaneous records of changes in membrane current and mag-indo-1 fluorescence (*left*) or indo-1 fluorescence (*right*) elicited by an application of CCh to the endplates of two muscle fibers. The top traces correspond to the CCh-induced change in membrane current. The middle series of traces corresponds to the fluorescence at 405 (F_{405}) and 470 nm (F_{470}), and the corresponding calculated $[Mg^{2+}]$ and $[Ca^{2+}]$ are shown at the bottom. Fibers were superfused with the 100 mM $MgSO_4$ external solution.

these conditions. Furthermore, as shown in the right panel of Fig. 6, CCh application to the endplate of a fiber that was pressure microinjected with the calcium indicator indo-1 failed to elicit any fluorescence response, although it induced a current similar to the one shown in the left panel. Considering the much higher affinity for calcium of indo-1 as compared to mag-indo-1 (Haugland, 1996), this result strongly argues against the possibility that the CCh-induced mag-indo-1 response would be due to an increase in $[Ca^{2+}]_i$. An in vitro calibration of the indo-1 response to magnesium was also performed, the results of which showed that, under our conditions, there was no change in the indo-1 fluorescence ratio between 0.1 and 200 mM $[Mg^{2+}]$ (not illustrated). Concerning the measured CCh-induced currents, it should be mentioned that the decay phase sometimes displayed a biphasic time course, as, for instance, in Fig. 5 (trace at −80 mV) and Fig. 6 (*left*). As previously suggested in other preparations, when observed, the initial decay phase was presumably due to the desensitization of the nicotinic receptors in the presence of the agonist, whereas the secondary faster decay phase reflected the closure of the channels after unbinding of the agonist (for a review, see Edmonds et al., 1995). Under our conditions, unbinding of CCh was determined by its dilution around the endplate due to the continuous superfusion of the high magnesium solution. It can also be noted in the right panel of Fig. 6 that the current trace displayed an intricate time course of activation. The origin of this complex activation was unclear and was not investigated further, as similar records were uncommon.

Fig. 7 shows a series of three consecutive (*from left to right*) CCh-induced responses elicited on the same fiber at 1-min intervals. The cell was pressure microinjected with mag-indo-1 and superfused with the 130 mM $MgSO_4$ external solution. The first and third responses were elicited by a 100-ms CCh puff to the endplate, whereas the second response (*middle column of traces*) was produced by a 500-ms CCh application. The first row shows the CCh-induced changes in membrane current. The second row presents what will be referred to as the theoretical change in $[Mg^{2+}]_i$: these transients were calculated from the running integral of the corresponding currents, assuming 1) that the CCh-induced currents are carried entirely by Mg^{2+}, and 2) that all of the Mg^{2+} entering the cell was readily available in a volume corresponding to the portion of the fiber from which fluorescence was measured. The third row shows the corresponding $[Mg^{2+}]_i$ traces calculated from the simultaneously measured mag-indo-1 fluorescence. Note that the *y* scale on the third row is expanded five times compared to the *y* scale of the traces shown on the second row. When we compare the respective corresponding currents and measured changes in $[Mg^{2+}]_i$, the results demonstrate that there was a clear dependence of the amplitude of the measured $[Mg^{2+}]_i$ change upon the amount of charge carried by the CCh-induced current. The two 100-ms puffs of CCh elicited currents of similar size and kinetics, and both induced a maximum change of $[Mg^{2+}]_i$ of ~0.2 mM. The 500-ms application of CCh induced a current of larger maximum amplitude and with a slower decaying phase, and the corresponding measured change in $[Mg^{2+}]_i$ was ~0.6 mM. Comparison of the second and third rows of traces shows that the maximum change in $[Mg^{2+}]_i$ was about five times smaller than expected, if all of the magnesium that entered the fiber would have appeared free in the cytoplasmic compartment.

Another example of successive CCh-induced responses is illustrated in Fig. 8. As in Fig. 7, the different rows show (*from top to bottom*) the CCh-induced changes in membrane

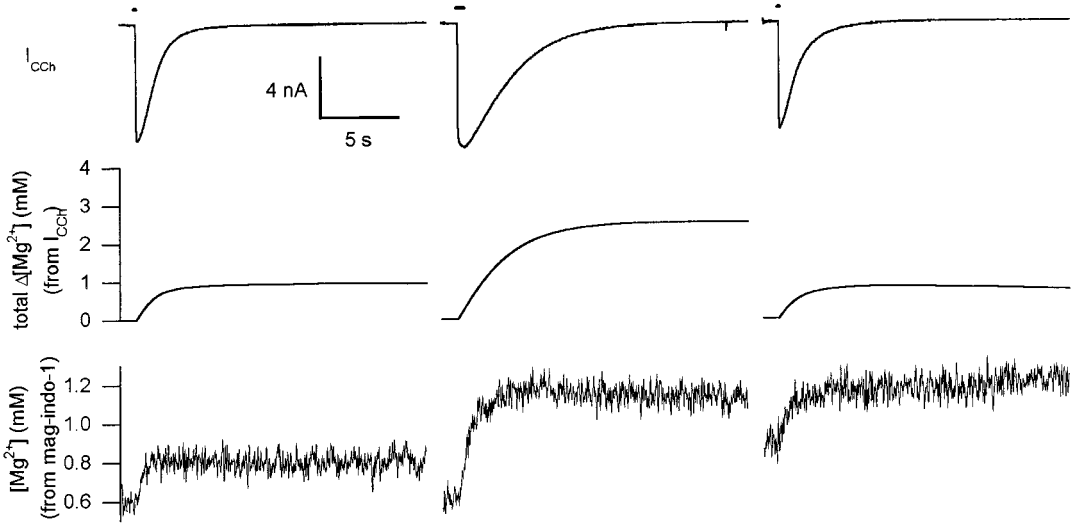

FIGURE 7 CCh-induced responses elicited on the same fiber, pressure microinjected with mag-indo-1 and superfused with the 130 mM $MgSO_4$ external solution. The injected solution contained (in mM) 140 K-aspartate, 1 mag-indo-1, 6 Hepes, 2 EGTA (pH 7.20). The first and third responses were elicited by a 100-ms CCh puff on the endplate, and the second response (*middle series of traces*) was produced by a 500-ms CCh puff. The first row shows the CCh-induced changes in membrane current; the second row shows the theoretical changes in $[Mg^{2+}]_i$ calculated from the running integral of the corresponding currents. The third row shows the corresponding $[Mg^{2+}]_i$ traces calculated from the mag-indo-1 fluorescence.

current, the corresponding theoretical changes in $[Mg^{2+}]_i$, and the measured $[Mg^{2+}]_i$, respectively. It should be noted that unlike in Fig. 7, the *y* scale amplitude is identical for the theoretical and measured $[Mg^{2+}]_i$. In the experiment presented in Fig. 8, although the results were qualitatively similar to those in Fig. 7, the theoretical CCh-induced changes in $[Mg^{2+}]_i$ were smaller, and surprisingly, the corresponding measured changes in $[Mg^{2+}]_i$ came much closer to the theoretical ones. For instance, the first and third responses yielded a theoretical change in $[Mg^{2+}]_i$ of ~0.3 mM, and the corresponding measured change in $[Mg^{2+}]_i$ was ~0.2 mM.

Measured versus theoretical change in $[Mg^{2+}]_i$

The overall results from simultaneous measurements of CCh-induced current and change in $[Mg^{2+}]_i$ performed on 10 distinct fibers are summarized in Fig. 9. Panels *A* and *B* of Fig. 9 show the same data presented in two different ways. Panel *A* shows the dependence of the measured maximum change in $[Mg^{2+}]_i$ upon the theoretical change, whereas panel *B* shows the ratio of the measured maximum change in $[Mg^{2+}]_i$ to the theoretical change in $[Mg^{2+}]_i$ versus the theoretical change. Different symbols correspond to different fibers. In panel *A*, results indicate that for all

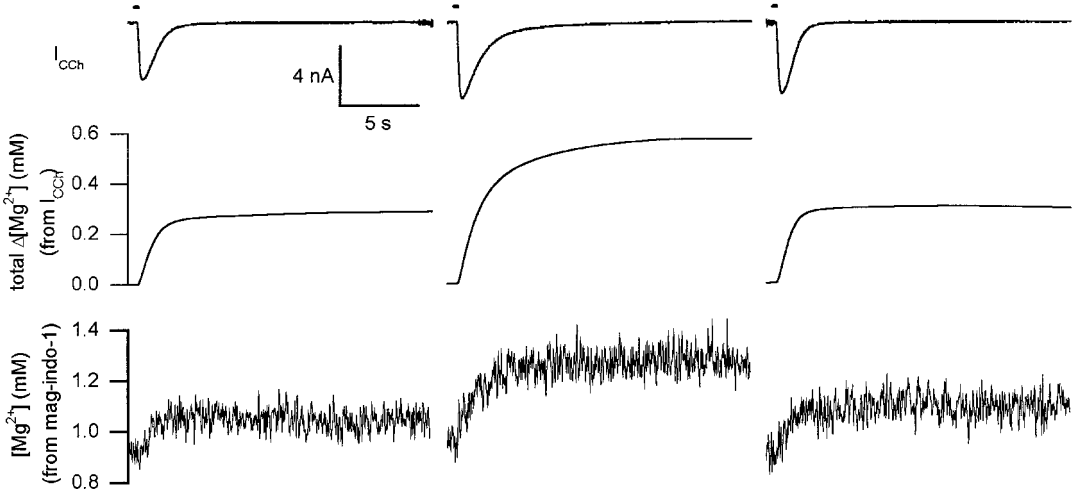

FIGURE 8 CCh-induced responses on a fiber, pressure microinjected with mag-indo-1 and superfused with the 130 mM $MgSO_4$ external solution. Experimental conditions were the same as in Fig. 7. Responses were elicited by 200-ms CCh puffs on the endplate. The first row shows the CCh-induced changes in membrane current; the second row shows the theoretical changes in $[Mg^{2+}]_i$ calculated from the running integral of the corresponding currents. The third row shows the corresponding $[Mg^{2+}]_i$ traces calculated from the simultaneously measured mag-indo-1 fluorescence.

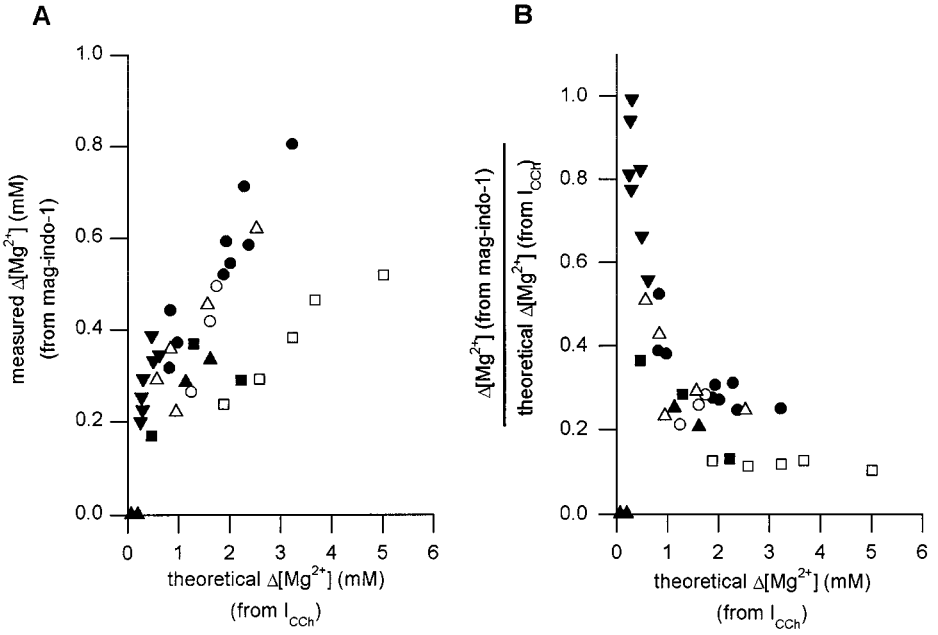

FIGURE 9 Dependence of the maximum change in $[Mg^{2+}]_i$ measured from the mag-indo-1 signals on the theoretical maximum change in $[Mg^{2+}]_i$ predicted from the integral of the CCh-induced membrane current. The different symbols correspond to distinct fibers. (*Left*) The maximum measured $\Delta[Mg^{2+}]_i$ versus the theoretical $\Delta[Mg^{2+}]_i$. (*Right*) The ratio of the measured $\Delta[Mg^{2+}]_i$ to the theoretical $\Delta[Mg^{2+}]_i$ versus the theoretical $\Delta[Mg^{2+}]_i$. △, ▲, ▼, Results from fibers superfused with the 100 mM $MgSO_4$ external solution; □, ■, ○, ●, results obtained with the 130 mM $MgSO_4$ external solution. The injected solution contained mag-indo-1 (1–2 mM) in 1) deionized water (○), 2) 100 mM K-aspartate, 30 mM K_2-ATP, 5 mM PIPES, 1 mM EGTA, pH 7.20 (□, ■, ●), 3) 115 mM K-aspartate, 10 mM EGTA, 8 mM HEPES, pH 7.20 (▲), 4) 140 mM K-aspartate, 2 mM EGTA, 6 HEPES, pH 7.20 (▼, △).

tested fibers, there was a clear tendency toward a concomitant increase in the measured and theoretical changes in $[Mg^{2+}]_i$. From panel *B*, results clearly show that for CCh currents that, according to our assumptions, would have increased the $[Mg^{2+}]_i$ by more than 1 mM, the maximum measured change in $[Mg^{2+}]_i$ was only 10–30% of the theoretical change. Conversely, for CCh currents that would have increased the $[Mg^{2+}]_i$ by less than 1 mM, results seem to indicate that the measured change in $[Mg^{2+}]_i$ tended to be closer to the theoretical one. Such a relationship between the measured change in free magnesium and the theoretical total change was unexpected, and would be hard to interpret simply in terms of intracellular magnesium buffering, because the effect of an intracellular magnesium buffer would be expected to induce an opposite relationship: the bigger the magnesium influx, the closer to 1 the ratio of the measured to the theoretical change in $[Mg^{2+}]_i$ should be as intracellular magnesium buffers become more saturated. Regarding this point, the results from three fibers injected with ATP and mag-indo-1 are included in Fig. 9. These ATP injections were originally performed to see whether we would be able to detect experimentally the presence of a higher concentration of a magnesium buffer from our measurements. In two of these fibers, the ATP concentration was estimated to be raised by ~7.5 mM from the injection (*open and filled squares*). For the third fiber (*closed circles*), the injected volume was not estimated. It then could be speculated that, in the graphs of Fig. 9, the positions of the opened squares as compared to the other data points indicate that, in that particular fiber, intracellular magnesium buffering had indeed been substantially raised by the ATP injection. However, the fit of the overall data with the predicted effect of magnesium buffering is so poor that it would be inappropriate to further analyze this effect. Finally, it should also be mentioned that no clear dependence was found between the measured change in $[Mg^{2+}]_i$ and the value of the resting $[Mg^{2+}]_i$ before the CCh application for similar theoretical changes in $[Mg^{2+}]_i$ (not shown).

DISCUSSION

Intracellular calibration of mag-indo-1

We developed an original method for calibrating the $[Mg^{2+}]$-dependent response of mag-indo-1 within isolated mouse skeletal muscle fibers. In muscular preparations, previous investigation of the intracellular response of ion-sensitive fluorescent dyes to $[Mg^{2+}]$ was achieved either through pressure microinjection of concentrated Mg-buffered solutions (Westerblad and Allen, 1992) or by equilibration of a known extracellular $[Mg^{2+}]$ across the plasma membrane by the use of ionophores (Silverman et al., 1994; Tashiro and Konishi, 1997). Our method was based upon the plasma membrane permeabilizing effect of saponin, which has been widely utilized on skeletal muscle to obtain the "skinned fiber" preparation and to perforate the plasma membrane of the ends of intact muscle fibers when mounted in a vaseline-gap device (Irving et al., 1987). In some respects, our approach, consisting of treating the isolated fibers with saponin in the presence of a calibrated Mg^{2+} solution as the extracellular medium, is similar to the one applied by Konishi and Watanabe (1995), who used β-escin to perform an intracellular calibration of the $[Ca^{2+}]$-dependent response of fura-dextran in frog skeletal muscle fibers. The main advantage of our method lies in the possibility of circumventing the loss of dye that normally occurs after the permeabilization process, by embedding the saponin-treated fibers in silicone grease before injecting mag-indo-1. The technique is not fully satisfactory, inasmuch as, in the period between permeabilization of the membrane and em-

bedding of the fibers, some intracellular components may already have leaked out of the fibers, which may change the dye response to $[Mg^{2+}]$. In addition, this effect may have been enhanced by the rather high concentration of saponin used (0.02%). This concentration was assessed to ensure the complete equilibration of intracellular $[Mg^{2+}]$ with the extracellular calibrated concentration before the fibers were embedded in silicone. Under these conditions, the loss of intracellular components represents an inherent drawback of the technique, the effects of which on the calibration are hard to evaluate. However, our results, showing that the mag-indo-1 calibration parameters were different in vivo and in vitro, indicate that the intracellular environment was sufficiently preserved to induce systematic changes in the properties of the dye. As compared to previous results obtained with furaptra in mouse skeletal muscle fibers, Westerblad and Allen (1992) reported no change in the values of R_{min}, R_{max}, and β from in vivo to in vitro, whereas the apparent affinity of the dye was slightly increased in vivo (by ~20%). On the other hand, in smooth muscle cells, Tashiro and Konishi (1997) reported that R_{min} for furaptra was unchanged in vivo as compared to in vitro, whereas R_{max} and K_D were increased by ~150% and 46%, respectively. Furthermore, Tashiro and Konishi (1997) did not observe any change in the wavelength dependence of the Mg-dependent intracellular fluorescence change as compared to in vitro, whereas our results suggest that the mag-indo-1 spectrum was modified in vivo. From our data, R_{min}, R_{max}, and β were increased in vivo by ~105%, 55%, and 140%, respectively, and we believe that the approximately twofold higher value of the binding constant ($K_D \cdot \beta$) that could be fitted to the in vivo data points may only result from the increase in β. Interestingly, the in vivo modifications of the mag-indo-1 calibration parameters observed here are analogous to those reported by Silverman et al. (1994) in isolated cardiac cells, where R_{min}, R_{max}, and $K_D \cdot \beta$ were increased by ~106%, 18%, and 66%, respectively. The difference between our results and those of Westerblad and Allen (1992) and Tashiro and Konishi (1997) may be related to different respective behaviors of mag-indo-1 and furaptra within the cytoplasmic environment. However, a difference in the respective amounts of binding of these two dyes to intracellular constituents is probably not the reason for the discrepancies, because binding was previously reported to be within the same range for these two dyes in frog skeletal muscle (Zaho et al., 1996). Again, it should be mentioned that, under our conditions, results from the calibration may have been partly influenced by the loss of intracellular constituents due to the saponin treatment.

Resting $[Mg^{2+}]_i$

Using the in vivo calibration parameters, the mean resting $[Mg^{2+}]_i$ was found to be ~1.5 mM for fibers bathed in regular Tyrode's solution. It may be stressed that this value is well below the apparent affinity of the dye for magnesium and that a higher affinity dye would be necessary for a more accurate determination of the resting $[Mg^{2+}]_i$. It is also important to note that, if one were to use the in vitro calibration parameters, this would yield a definitely higher calculated mean resting $[Mg^{2+}]_i$ (2.5 mM), which emphasizes the importance of performing an intracellular calibration of the dye response. For comparison with previous studies, considering the wide range of resting $[Mg^{2+}]_i$ values found in the literature for skeletal muscle preparations, there is no doubt that we could find and/or refer to data that would match those of the present study. If we just restrict the comparison to studies performed on mammalian skeletal muscle, our estimate of the resting $[Mg^{2+}]_i$ lies between the value reported by Alamo et al. (1986) in rabbit skeletal muscle, measured using $[Mg^{2+}]$-sensitive microelectrodes (3.7 mM), and the ones reported by MacDermott (1990) for rat extensor digitorum muscle, also measured using $[Mg^{2+}]$-sensitive microelectrodes (0.47 mM), and Westerblad and Allen (1992) for mouse skeletal muscle fibers, using furaptra (0.78 mM), respectively. The value reported by Alamo et al. (1986) was probably an overestimation due to the interference of the $[Mg^{2+}]$-sensitive microelectrodes with K^+ and Na^+, which was not precisely taken into account (see, for instance, Blatter, 1990). On the other hand, the discrepancy with the results of MacDermott (1990) and Westerblad and Allen (1992) is unclear and may be related to specific differences in the conditions in which the experiments were performed.

CCh-induced responses

We were able to detect changes in intracellular $[Mg^{2+}]$ due to Mg entry through the nicotinic receptors at the endplate of the isolated fibers. On the same fiber, the maximum amplitude of the $[Mg^{2+}]_i$ increase was qualitatively consistent with the amount of charge carried by the CCh-induced current, i.e., the greater the charge carried by the current, the larger the amplitude of the $[Mg^{2+}]_i$ increase. However, the overall quantitative comparison of the theoretical total change and measured free change in magnesium from distinct fibers gave unexpected results. For currents that should have induced a theoretical total $[Mg^{2+}]$ increase of less than ~1 mM, it seemed that the smaller the amount of Mg that entered the cell, the closer to 1 the ratio of the measured to the theoretical change in $[Mg^{2+}]_i$ would be. On the other hand, for larger amounts of Mg entering the cell, the ratio of the measured to the theoretical change in $[Mg^{2+}]_i$ was down to ~0.1–0.3. This relationship between the measured and theoretical changes in $[Mg^{2+}]_i$ appears to be inconsistent with the simple effect of intracellular Mg buffers, and in this regard we failed in our attempt to directly assess the intracellular Mg buffering power from these experiments. The possibility that the CCh-induced currents measured here were not essentially carried by Mg^{2+} ions should be considered. It is highly unlikely that a chloride conductance interfered with our measurements, as the permeability of

anions through endplate channels is negligibly low, and, to our knowledge, there is no indication in the literature that Cl^- ions could go through any other CCh-induced pathway on this preparation under the present conditions. Conversely, if an outward current of cations had interfered, the Mg^{2+} entry would then have been underestimated, and therefore, the discrepancy between measured and predicted changes in $[Mg^{2+}]$ would also have been underestimated. From a more general point of view, it may be emphasized that the possibility that any CCh-induced conductance, other than that carried by Mg^{2+} ions, contaminated our measurements in such way that it could be responsible for the inconsistency between measured and predicted $\Delta[Mg^{2+}]$, would require that the proportion of the non-Mg^{2+} component would depend on the amount of charge carried by the whole current, which is not readily conceivable. Rather, we tend to think that other kinds of uncertainties/artifacts may be responsible for the inconsistency between predicted and measured $\Delta[Mg^{2+}]$. In particular, our estimation of the theoretical total change in $[Mg^{2+}]_i$ may be erroneous because of the fact that, in our conditions, magnesium entering the fiber could not only be trapped by intracellular magnesium buffers, but could also diffuse within the fiber, out of the field of fluorescence measurement, and thus become diluted in a larger volume of fiber than assumed here. Regarding this possibility, it may be stressed that, over the recorded interval, we never observed any clear decay of the measured change in $[Mg^{2+}]_i$ after the end of the CCh-induced current, which indicates that intracellular Mg^{2+} diffusion may not strongly interfere. In any case, quantitative investigation of this possibility would require precise knowledge of the Mg diffusion constant within the cytoplasm, the value of which, to our knowledge, is not clearly established. On the other hand, it may also be that, in our conditions, the measured fluorescence signals arise from a strongly inhomogeneous CCh-induced change in $[Mg^{2+}]_i$ due to the restricted membrane area from which Mg entry occurs. A preliminary simulation assuming intracellular Mg diffusion to be very slow suggests that local accumulation of $[Mg^{2+}]_i$ associated with local saturation of the dye could account for the observed results (not illustrated). However, further quantitative investigation of that possibility would again require some knowledge about Mg^{2+} diffusion within the intracellular environment.

In conclusion, we established a new efficient method for calibrating the intracellular response of mag-indo-1 in skeletal muscle fibers, and the procedure we used should also be appropriate for calibrating the intracellular response of other ion-sensitive fluorescent dyes. The resting $[Mg^{2+}]_i$ in mouse skeletal muscle fibers was found to be $\sim$1.5 mM, and our combined measurements of a Mg entry through the nicotinic receptors, together with $[Mg^{2+}]_i$, demonstrated that mag-indo-1 can be reliably used to quantitatively track $[Mg^{2+}]_i$ changes in skeletal muscle fibers.

We thank Drs. Bruno Allard, Carlos Ojeda, Yves Tourneur, and Oger Rougier for helpful discussions while we prepared this paper.

This study was supported by the Centre National de la Recherche Scientifique (CNRS), the Université Claude Bernard, and a grant from the Région Rhône-Alpes. The visits of Dr. Csernoch to Lyon were financed by the French/Hungarian intergovernmental program Balaton (95011, 95012).

REFERENCES

Adams, D. J., T. M. Dwyer, and B. Hille. 1980. The permeability of endplate channels to monovalent and divalent metal cations. *J. Gen. Physiol.* 75:493–510.

Agus, Z. S., and M. Morad. 1991. Modulation of cardiac ion channels by magnesium. *Annu. Rev. Physiol.* 53:299–307.

Alamo, L., J. R. Lopez, L. Papp, and F. A. Streter. 1986. Simultaneous measurement by means of ion-specific electrodes of free intracellular ionized calcium and magnesium in rabbit skeletal muscle. *Muscle Nerve.* 9:472–474.

Allard, B., J. C. Bernengo, O. Rougier, and V. Jacquemond. 1996. Intracellular Ca^{2+} changes and Ca^{2+}-activated K^+ channels activation induced by acetylcholine at the endplate of mouse skeletal muscle fibers. *J. Physiol. (Lond.).* 494:337–349.

Bakker, A. J., S. I. Head, D. A. Williams, and D. G. Stephenson. 1993. Ca^{2+} levels in myotubes grown from the skeletal muscle of dystrophic (mdx) and normal mice. *J. Physiol. (Lond.).* 460:1–13.

Bernengo, J. C., H. Sun, and F. Jacquey. 1992. Application of microspectrophotometry to cytoplasmic free magnesium concentration determination in cultured cells. *J. Cell. Pharmacol.* 3:111–119.

Blatter, L. A. 1990. Intracellular free magnesium in frog skeletal muscle studied with a new type of magnesium-selective microelectrode: interactions between magnesium and sodium in the regulation of $[Mg]_i$. *Pflügers Arch.* 416:238–246.

Csernoch, L., J. C. Bernengo, and V. Jacquemond. 1996. Measurements of free intracellular magnesium concentration ($[Mg^{++}]_i$) using the fluorescent indicator mag-indo-1 in isolated mouse skeletal muscle fibers. *Biophys. J.* 270:A169.

Edmonds, B., A. J. Gibb, and D. Colquhoun. 1995. Mechanisms of activation of muscle nicotinic acetylcholine receptors and the time course of endplate currents. *Annu. Rev. Physiol.* 57:469–493.

Gillis, J. M., D. Thomason, J. Lefèvre, and R. H. Kretsinger. 1982. Parvalbumins and muscle relaxation: a computer simulation study. *J. Muscle Res. Cell Motil.* 3:377–398.

Grynkiewicz, G., M. Poenie, and R. Y. Tsien. 1985. A new generation of Ca^{2+} indicators with greatly improved fluorescence properties. *J. Biol. Chem.* 260:3440–3450.

Haugland, R. P. 1996. Handbook of Fluorescent Probes and Research Chemicals, 6th Ed. Molecular Probes, Eugene, OR.

Hou, T., J. D. Johnson, and J. A. Rall. 1991. Parvalbumin content and Ca^{2+} and Mg^{2+} dissociation rates correlated with changes in relaxation rate of frog muscle fibres. *J. Gen. Physiol.* 441:285–304.

Irving, M., J. Maylie, N. L. Sizto, and W. K. Chandler. 1987. Intrinsic optical and passive electrical properties of cut frog twitch fibers. *J. Gen. Physiol.* 89:1–40.

Irving, M., J. Maylie, N. L. Sizto, and W. K. Chandler. 1989. Simultaneous monitoring of changes in magnesium and calcium concentrations in frog cut twitch fibers containing antipyrylazo III. *J. Gen. Physiol.* 93: 585–608.

Jacquemond, V. 1997. Indo-1 fluorescence signals elicited by membrane depolarization in enzymatically isolated mouse skeletal muscle fibers. *Biophys. J.* 73:920–928.

Jacquemond, V., and M. F. Schneider. 1992a. Effects of low myoplasmic Mg^{2+} on calcium binding by parvalbumin and calcium uptake by the sarcoplasmic reticulum in frog skeletal muscle. *J. Gen. Physiol.* 100: 115–135.

Jacquemond, V., and M. F. Schneider. 1992b. Low myoplasmic Mg^{2+} potentiates calcium release during depolarization of frog skeletal muscle fibers. *J. Gen. Physiol.* 100:137–154.

Kabbara, A. A., and D. G. Stephenson. 1994. Effects of Mg^{2+} on Ca^{2+} handling by the sarcoplasmic reticulum in skinned skeletal and cardiac muscle fibres. *Pflügers Arch.* 428:331–339.

Konishi, M., N. Suda, and S. Kurihara. 1993. Fluorescence signals from the Mg^{2+}/Ca^{2+} indicator furaptra in frog skeletal muscle fibers. *Biophys. J.* 64:223–239.

Konishi, M., and M. Watanabe. 1995. Resting cytoplasmic free Ca^{2+} concentration in frog skeletal muscle measured with fura-2 conjugated to high molecular weight dextran. *J. Gen. Physiol.* 106:1123–1150.

Lamb, G. D., and D. G. Stephenson. 1991. Effect of Mg^{2+} on the control of Ca^{2+} release in skeletal muscle fibres of the toad. *J. Physiol. (Lond.).* 434:507–528.

MacDermott, M. 1990. The intracellular concentration of free magnesium in extensor digitorum longus muscles of the rat. *Exp. Physiol.* 75: 763–769.

Manthey, A. M. 1995. Interaction of Na^{+} and Mg^{2+} ions in acetylcholine receptor channels of frog skeletal muscle changes in character with an increase in agonist concentration. *Pflügers Arch.* 430:894–900.

Potter, J. D., S. P. Robertson, and J. D. Johnson. 1981. Magnesium and the regulation of muscle contraction. *Fed. Proc.* 40:2653–2656.

Romani, A., and A. Scarpa. 1992. Regulation of cell magnesium. *Arch. Biochem. Biophys.* 298:1–12.

Silverman, H. S., F. Di Lisa, R. C. Hui, H. Miyata, S. J. Sollott, R. G. Hansford, E. G. Lakatta, and M. D. Stern. 1994. Regulation of intracellular free Mg^{2+} and contraction in single adult mammalian cardiac myocytes. *Am. J. Physiol.* 266:C222–C233.

Stephenson, E. W. 1981. Magnesium effects on activation of skinned fibers from striated muscle. *Fed. Proc.* 40:2662–2666.

Tashiro, M., and M. Konishi. 1997. Basal intracellular free Mg^{2+} concentration in smooth muscle cells of guinea pig tenia cecum: intracellular calibration of the fluorescent indicator furaptra. *Biophys. J.* 73: 3358–3370.

Vranesic, I., and T. Knöpfel. 1991. Calculation of calcium dynamics from single wavelength fura-2 fluorescence recordings. *Pflügers Arch.* 418: 184–189.

Westerblad, H., and D. G. Allen. 1992. Myoplasmic free Mg^{2+} concentration during repetitive stimulation of single fibres from mouse skeletal muscle. *J. Physiol. (Lond.).* 453:413–434.

Westerblad, H., and D. G. Allen. 1996. Intracellular calibration of the calcium indicator indo-1 in isolated fibers of *Xenopus* muscle. *Biophys. J.* 71:908–917.

Zaho, S., S. Hollingworth, and S. M. Baylor. 1996. Properties of tri- and tetracarboxylate Ca^{2+} indicators in frog skeletal muscle fibers. *Biophys. J.* 70:896–916.